



**HAL**  
open science

## Effect of Process Parameters on the Properties of Direct Written gas-generating Reactive Layers

Florent Sevely, Xuwen Liu, Tao Wu, Fabien Mesnilgrete, Bernard Franc, Sandrine Assié-Souleille, Xavier Dollat, Carole Rossi

► **To cite this version:**

Florent Sevely, Xuwen Liu, Tao Wu, Fabien Mesnilgrete, Bernard Franc, et al.. Effect of Process Parameters on the Properties of Direct Written gas-generating Reactive Layers. ACS Applied Polymer Materials, 2021, 3 (8), pp.3972-3980. 10.1021/acsapm.1c00513 . hal-03302390

**HAL Id: hal-03302390**

**<https://laas.hal.science/hal-03302390>**

Submitted on 27 Jul 2021

**HAL** is a multi-disciplinary open access archive for the deposit and dissemination of scientific research documents, whether they are published or not. The documents may come from teaching and research institutions in France or abroad, or from public or private research centers.

L'archive ouverte pluridisciplinaire **HAL**, est destinée au dépôt et à la diffusion de documents scientifiques de niveau recherche, publiés ou non, émanant des établissements d'enseignement et de recherche français ou étrangers, des laboratoires publics ou privés.

# Effect of Process Parameters on the Properties of Direct Written gas-generating Reactive Layers

*Florent Sevely<sup>1</sup>, Xuwen Liu<sup>1,2</sup>, Tao Wu<sup>1</sup>, Fabien Mesnilgrete<sup>1</sup>, Bernard Franc<sup>1</sup>, Sandrine Assie-Souleille<sup>1</sup>, Xavier Dollat<sup>1</sup>, Carole Rossi<sup>1,\*</sup>*

<sup>1</sup> LAAS-CNRS, University of Toulouse, 7 Avenue du colonel Roche, 31400 Toulouse, France

<sup>2</sup> School of Chemical Engineering, Nanjing University of Science and Technology, 200 Xiaolingwei Street, Nanjing 210094, China

KEYWORDS: reactive material, 3D printing, thermite, gas generation, energetic materials, direct writing

## ABSTRACT

A mixture of copper complex and Al/CuO nanothermite, Al/CuO/CuC, represents one state-of-the-art gas-generating thermite systems with various pyrotechnic applications with respect to their tunable gas release rates. The reactivity of reactive inks with various loading of polyvinylpyrrolidone (PVP) binder mixed with Al/CuO/CuC is characterized using high-speed imaging diagnostics and pressure measurement. For a PVP mass fraction < 7 wt%, the printed materials remain highly reactive and burn at a high velocity (10 – 54 m/s) which was one of the important goals in this study. At higher PVP content, the polymer inhibits the reaction. Printing (dropwise and continuously writing) of inks containing 5 wt% of PVP and 95 wt% of reactive Al/CuO/CuC powder was demonstrated using volumetrically controlled dispenser and pneumatically actuated syringe. The pressure development and burning rates of the printed materials are 0.37 MPa (at 46.3% TMD) and 17 m/s (at 0.24% TMD), more than a 10 times faster than the majority of works dealing with printed energetic formulations.

## TEXT

### 1. Introduction

Nanothermites, consisting of a metal fuel and a metal oxide both in nanoscale (the order of 100 nm or less), have been extensively investigated for a large variety of formulations (Al/CuO, Al/Fe<sub>2</sub>O<sub>3</sub>, Al/MoO<sub>3</sub>, etc) <sup>1-5</sup> and developed for use in welding and joining, propulsion <sup>6-8</sup> and propellant rate modifier <sup>9</sup>, heat source applications <sup>10, 11</sup>, as well as micro-energetics. <sup>12-14</sup> For practical use in many applications, loose powder may not be suitable, and the thermite must be either pressed or mixed with a binder to form contiguous layer of reactive materials. In the last decade, the main focus for printing reactive materials has been inkjet <sup>15-17</sup>, vapor deposition <sup>18-20</sup>, or spray technologies <sup>21</sup>. Although all these techniques are viable and efficient methods to engineer thin reactive film, they present limitations in their application: they are well adapted to thin film deposition but not suitable to engineer structures of varying three-dimensional (3D)

geometries; they present scale-up limitations and often additional processing steps are required after deposition to achieve structural integrity. Direct-writing of solvent based thermite inks appear to be a good alternative method to deposit thick reactive layers with varying sub-millimeter features<sup>22-26</sup>. Not only it is a fast and simple technique, but the safety during processing is improved by the presence of the solvent. Sullivan et al.<sup>25,27</sup> and Murray et al.<sup>16</sup> have both presented first technological demonstrations of 3D printed reactive materials and explored direct-writing or 3D printing to tailor the energy release and combustion performance by architecting the reactive film at the microscale. For example, Sullivan et al.<sup>27</sup> succeeded in tuning burn rate in the range of 1-10 m/s, in 3D-printed Al/CuO thermite by printing void channels inside the film. Mao et al.<sup>28</sup> printed Al/CuO thermite with micro-architected patterns that also showed tunable burning rate ranging from 3 to 35 cm/s. Not only the printing architecture impacts the energy release and combustion performance, but also the binder, even though it is added in the minimum quantity necessary to provide structural integrity to the thermite formulations and afford stable reactive films, plays an important role in particle mixing, deposition thickness, and density, all of which affecting the flame temperature, burn rate, and energy release rate. Groven et al.<sup>29</sup> and Son et al.<sup>16,30,31</sup> have both shown success in printing fluoropolymer-based reactive material. Meeks et al.<sup>32</sup> successfully synthesized and characterized the burn rate of thick Mg/MnO<sub>2</sub> thermite films mixed with different binders (PolyvinylideneFluoride (PVDF) – Methyl Pyrrolidone (NMP); Vitonfluoroelastomer (Viton A)). Results showed that both the binder type and concentration influence the film combustion behaviour. Considering Viton binder, burn rates decrease with increasing binder concentration, with a maximum of 0.14 m/s<sup>32</sup>. Using a polyvinylidene fluoride (PVDF) binder gives the highest burn rates (0.15 m/s) which Meeks et al. attributed to a more homogenous distribution of the reactants in the film. Another study<sup>33</sup> has incorporated thermite into the common 3D printing polymers, acrylonitrile butadiene styrene (ABS), and has found a maximum burn rate

of 1.21 cm/s at 20 wt% ABS. Shen et al. successfully synthesized and characterized the burn rate of an Al/CuO nanothermite ink with particle loading as high as 90 wt% mixed in a PVDF (4 wt%) and hydroxy propyl methyl cellulose (HPMC) (6 wt%)<sup>34</sup>. The burn rate of the printed films is ~2–10 cm/s, with flame temperatures of ~2800 K. Faster burn rates (up to 25 cm/s) are found when PVDF is replaced by nitrocellulose and polystyrene<sup>35</sup>. Interestingly, with well-chosen binders, all studies produced stable, safe and printable reactive materials that have the potential to be printed or written on any devices or substrates but all produced slow to moderate burning rates i.e. on the order of cm/s, almost two decades lower than burn rate measured using loose thermite powders<sup>3</sup>. Low burning rate characteristic is not a difficulty for propulsion applications but constitutes a limitation for other applications requiring highly reactive materials to ensure the flame propagation.

The primary focus of this work is therefore to engineer printable reactive layers with high burn rates (> 10 m/s) notably for micro-energetic application such as chip destruction that requires large energy output and gaseous production within a short time. Recently, copper complex,  $\text{Cu}(\text{NH}_3)_4(\text{NO}_3)_2$  (referred to as CuC in this paper), selected for its propensity to generate non-toxic gases (0.03 mol/g of  $\text{N}_2$ ,  $\text{NH}_3$ ,  $\text{H}_2\text{O}$ ,  $\text{N}_2\text{O}$ ) through exothermic chemical decomposition (300 J/g), were mixed with Al/CuO nanothermites to produce a highly-reactive gas generating composite<sup>36</sup>. The presence of CuC over Al/CuO in a 1:3 mass ratio permits to achieve a pressure development (in close bomb) and burn rate (unconfined) ~5 and 2 times higher than sole Al/CuO thermite mixture, respectively<sup>37</sup>. However, in powder form, this reactive mixture is inconvenient to be integrated onto or into a miniaturized device. The main technical objectives of this study are three-fold: first to develop a stable Al/CuO/CuC reactive inks using various concentrations of polymeric PVP binder. PVP was chosen as it is commonly used in materials preparation and MEMS technologies<sup>38, 39</sup> and presents the advantage to be biocompatible<sup>40</sup>. Second, to investigate the influence of PVP mass fraction on the combustion

performances of the printed materials. Third, to demonstrate and characterize the printing (dropwise and continuously writing) produced by two writing methods: volumetrically controlled dispenser and pneumatically actuated syringe. As final results, a stable ink with 5 wt% of PVP polymer and 95 wt% Al/CuO/CuC powder was optimized that can be printed in contiguous layer by a simple direct-writing method. The pressure development and burning rates of the prepared materials are 0.37 MPa (for a very low compaction of 0.06 g/cm<sup>3</sup>) and 17 m/s *i.e.* more than a decade faster than the majority of works dealing with printed energetic formulations featuring combustion speed well below 1 m/s.

## **2. Experimental section**

### **2.1. Materials**

The aluminum nanopowders (Al, average particle size: 80 nm, purity: 69%) were purchased from Novacentrix (USA) and stored in a glove box for future uses. Copper oxide (CuO, average particle size: 100 nm), copper nitrate trihydrate, 25% aqueous ammonia, ethanol (CH<sub>3</sub>CH<sub>2</sub>OH, anhydrous, 99.9%), and polyvinylpyrrolidone (PVP, molar weight: 40k) purchased from Merck (Germany) were directly used as received. CuC was synthesized according to a previous published method<sup>36</sup>. In brief, 4.83 g (0.02 mol) of copper nitrate trihydrate was dissolved in 10 mL of distilled water followed by addition of 15 mL of 25% aqueous ammonia solution (0.24 mol). The final powder was separated via vacuum filtration and dried in an oven (Carbolite Gero, England) at 70 °C. Materials description is listed in **Table S1**.

### **2.2. Thermite mixtures and reactive inks preparations**

To prepare Al/CuO nanothermite, 114 mg of Al powder and 286 mg of CuO were dispersed in ethanol and then stirred for 45 minutes in a sonication bath cooled by ice. The suspension was then dried at 50 °C. The dry powder (referred to as Al/CuO<sub>ref</sub>) was collected and reserved for

future use. Note that the masses of Al and CuO were calculated based on an equivalence ratio of 1.2.

To prepare Al/CuO/CuC reactive mixture, Al (96 mg), CuO (214 mg) and CuC (90 mg) were mixed following the same procedure as for Al/CuO. The equivalence ratio for Al/CuO was kept at 1.2 and the CuC over Al/CuO ratio is 33 wt%. The dry powder (referred to as TC\_ref) was then collected and stored in vials for future use.

To prepare Al/CuO/CuC/PVP reactive inks, PVP was first dissolved in ethanol (PVP/ethanol 5 wt%) and sonicated for a certain amount of time till it is fully dissolved. Next, the Al/CuO\_ref and TC\_ref dry powders were mixed with PVP solution followed by 45 minutes sonication. The obtained solution was then sealed in a 10 mL glass vial and reserved for characterizations. The chemical compositions of each prepared mixture are listed in **Table 1**. For clarity, the following labelling was chosen: TC\_#%, with TC refers to Al/CuO/CuC reactive mixture and #% indicates the mass fraction of PVP in the mixture. As an example, TC\_5% means that the composite contains 5% of PVP and 95% of Al/CuO/CuC in mass.

**Table 1.** Reactive mixtures prepared for this study detailing their composition.

Thermite Materials	PVP mass (mg) wt%	Al (mg)	CuO (mg)	CuC (mg)	Ethanol (ml)
Al/CuO_ref	No PVP	114	286	0	4
Al/CuO_5%	PVP (20) 5 %	108	272	0	4
TC_ref	No PVP	96	214	90	4
TC_3%	PVP (12) 3%	93	208	87	4
TC_5%	PVP (20) 5%	91	203	86	4
TC_7%	PVP (28) 7%	89	199	84	4

TC_10%	PVP (40) 10%	86	193	81	4
TC_15%	PVP (60) 15%	82	182	76	4
TC_20%	PVP (80) 20%	77	171	72	4
TC_25%	PVP (100) 25%	72	160	68	4

**Figure 1a** presents a schematic of the preparation of reactive inks. Then, the writing of prepared inks was done using either a pneumatically actuated syringe (**Figure 1b**) or a volumetrically controlled dispenser (**Figure 1c**). The writing patterns are controlled precisely by regulating the ink output using injection parameters: pressure (0.3 bar) and application time (0.25 s) in pneumatically actuated syringe apparatus and volume (6  $\mu$ L) for the volumetrically controlled dispenser.

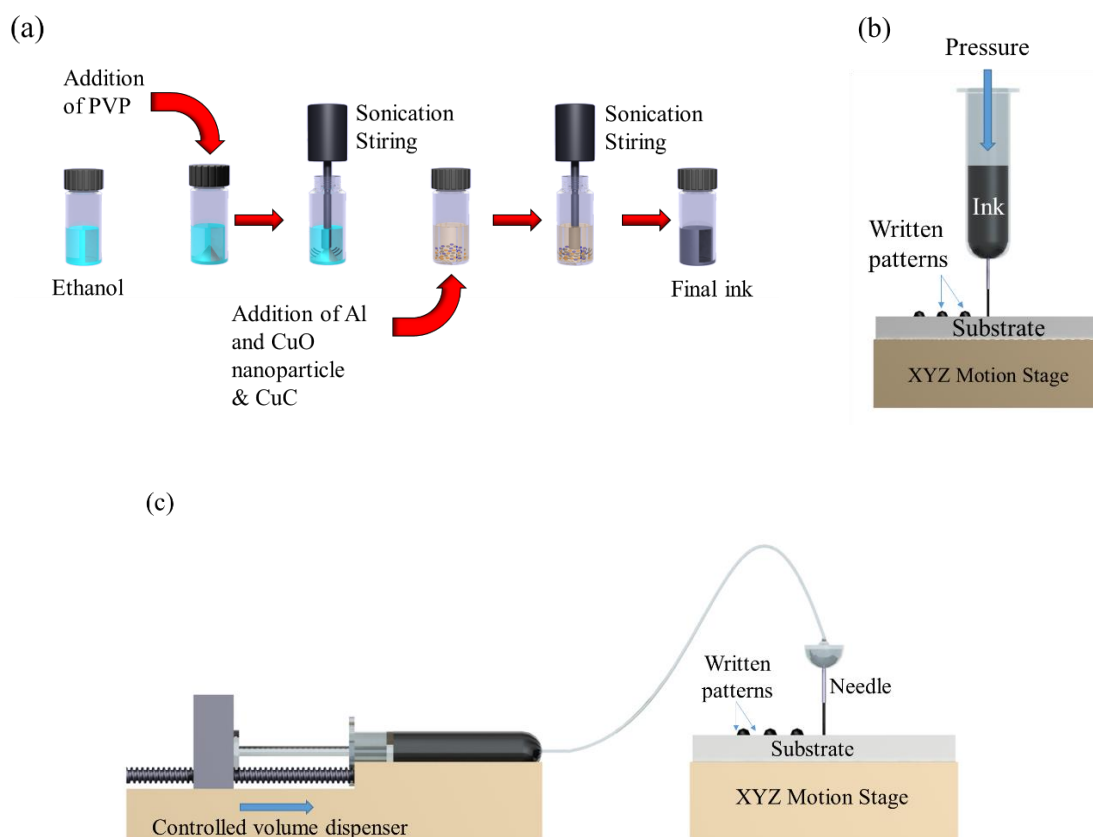


**Figure 1.** Schematic of (a) the thermite composites and inks preparation and direct-writing methods with (b) a simplest pneumatically actuated syringe, and with (c) the volumetrically controlled dispenser.

### 2.3. Experimental methods

The viscosity of the ink was measured using an Anton Paar AMVn viscometer and a 1.6 mm capillary at ambient temperature (25 °C). Two sensors in the equipment measure the falling time of a perfect metal ball in the capillary using different tilt angle. This time is compared with the falling time in water while taking the water viscosity (1 mPa.s) as reference.

The morphology and particle sizes of obtained reactive layers (dried inks) were observed by scanning electronic microscopy (SEM) using a Hitachi S-4800 (cold FEG) operating at 2.0 kV.

The pressure data were acquired by a high-frequency pressure transducer (Kistler 6215 type) : for all tests, about ~13 mg of materials were printed in a annular mold<sup>37</sup> and placed in a stainless steel and high pressure resistant cylindrical reactor<sup>36,41</sup> which has a total volume of ~200 mm<sup>3</sup> (details in **Figure S1**). The final packing density of reactive materials inside the bomb is calculated at 1.625 g/cm<sup>3</sup> ~ 46.3% TMD (Theoretical Maximun Density).

The mean linear burn rate was recorded using a high-speed camera Photon SA3 at a speed of 75,000 frames per second, with a 128 × 32 images resolution : a printed line of each materials were deposited in polycarbonate mold (trench of 30 mm long, 1 mm wide and 1 mm deep)<sup>44</sup> and ignited at one end with a pyroMEMS<sup>14</sup>. The density of the reactive material inside the mold was evaluated to be at 0.08 g/cm<sup>3</sup> ~0.24% TMD. In parallel, the optical emission spectrum produced by the combustion is captured by an optical fiber and recorded by a spectrometer (AvaSpecULS2048CL-EVO spectrometer, Avantes Inc.). A 6 mm diameter collimating lens (confocal length 8.7 mm) is placed at approximately 40 mm from the propagating front to capture light. The system is calibrated using a HG-1 mercury-argon calibration source from

Ocean Optics, Inc. **Figure S2** shows the experimental setup scheme employed in the combustion experiments. A multi-wave pyrometry method was then used to calculate the flame temperature. The method is similar to that first reported by Ng and Fralick<sup>42</sup> and further detailed in<sup>13</sup>. In brief, considering that the flame is mainly composed of an aluminum oxide particles cloud at temperature,  $T$ , near 3000 K, the emissivity,  $\varepsilon$ , is assumed to be independent of the wavelength (greybody assumption). Therefore, the Planck's distribution can be written as in Equation 1.

$$\ln \left[ \frac{2\pi hc_0^2}{\lambda^5 L} \right] = \frac{hc_0}{k_B \lambda T} + \ln \left[ 1 - \exp \left( -\frac{hc_0}{k_B \lambda T} \right) \right] - \ln \varepsilon \quad (1)$$

With

- $L$ , emitted radiation intensity,
- $\lambda$ , wavelength,
- $h$  is the Planck's constant,
- $c_0$  is the speed of light in vacuum,
- $k_B$  is the Boltzmann constant,

Then, plotting:

$$\frac{\ln \left[ \frac{2\pi hc_0^2}{\lambda^5 L} \right]}{\frac{hc_0}{k_B \lambda}}$$

as a function of  $\lambda$  is a straight line with a slope of:

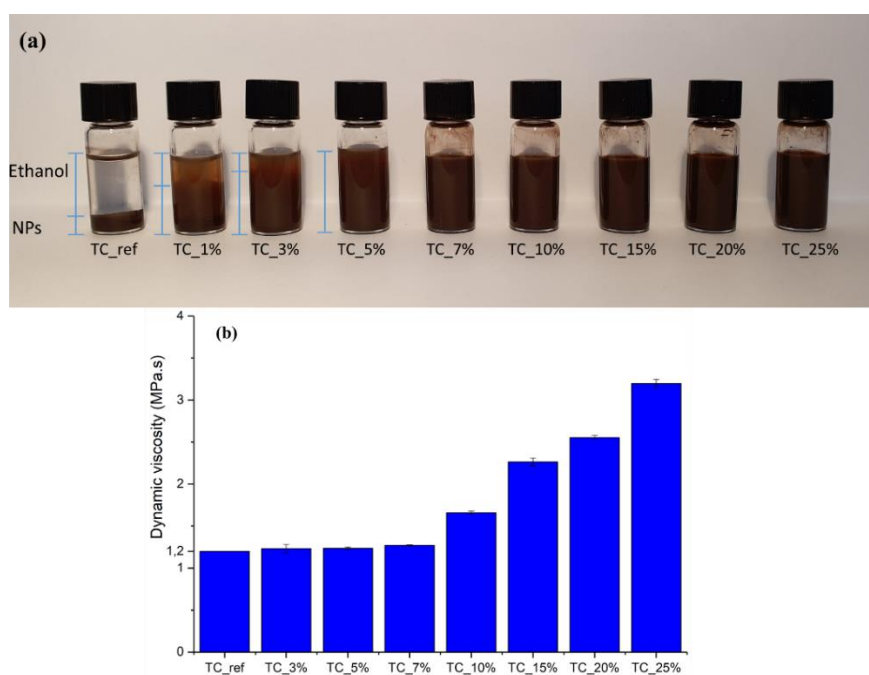
$$\frac{-k_B \ln \varepsilon}{hc_0}$$

The spectral range of 400 – 800 nm was used for this analysis as it features the best detector efficiency.

### 3. Results and Discussion

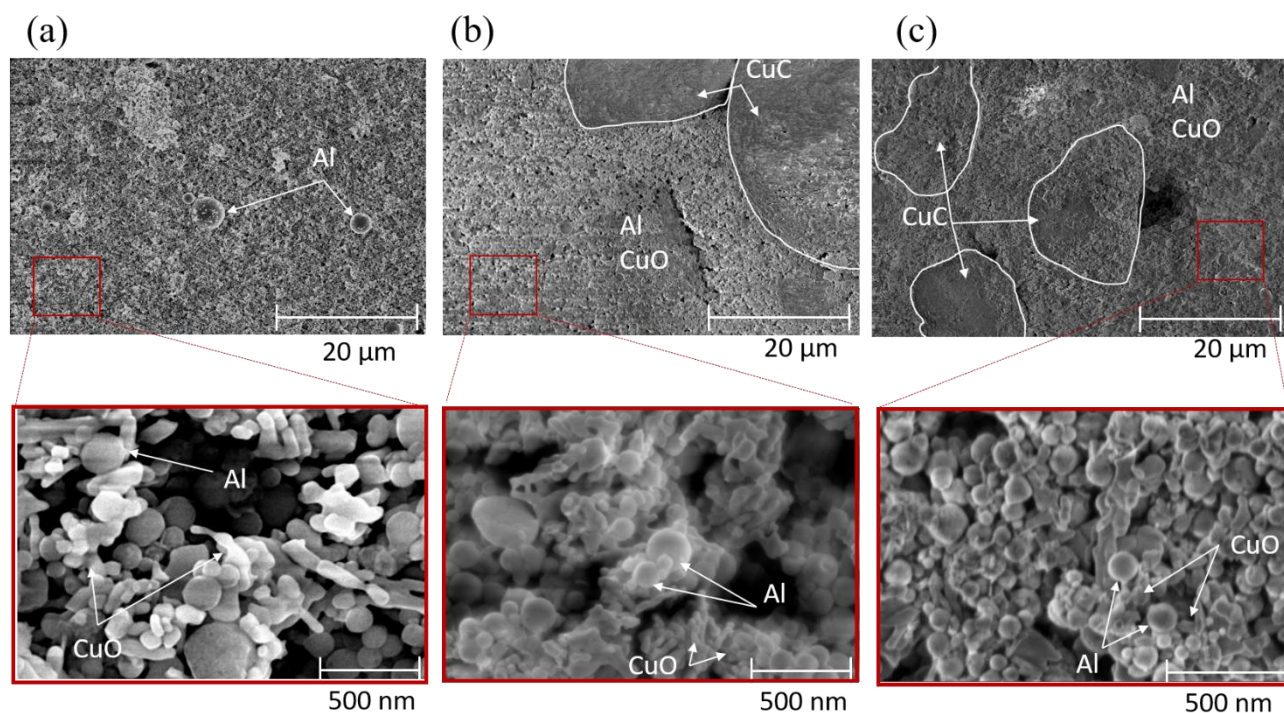
#### 3.1. Reactive inks characterization

The addition of PVP does not increase the viscosity beyond 3.2 mPa.s, which means that the inks remain in liquid as long as the content of PVP < 25 wt%. As references, viscosity of ethanol and water is 1.2 mPa.s and 1 mPa.s, respectively. **Figure 2a** exhibits optical images of the prepared inks, *i.e.* TC\_ref, TC\_1%, TC\_3%, TC\_5%, TC\_7%, TC\_10%, TC\_15%, TC\_20%, TC\_25%, after 24 hours storage at room temperature. Without PVP, all particles precipitate to the bottom of the vial after less than 1 hour. Adding  $\geq 5$  wt% of polymers stabilize the ink for 24 h. After one full day, the particles precipitate and the suspension needs to be re-stirred 10 min in a sonication bath before printing. **Figure 2b** plots the viscosity of solutions as a function of the binder content. For less than 7 wt% of polymer, the impact on the viscosity is almost null, at 20 wt% of polymer, the viscosity is almost the double of the ethanol viscosity value.



**Figure 2.** (a) Photographs of the vials containing the different prepared reactive inks after 24 h of storage at ambient and, (b) dynamic viscosity as a function of the PVP content.

**Figure 3** displays SEM images of four dried reactive inks: TC\_3%, TC\_5%, TC\_10%, TC\_25% in comparison with Al/CuO\_ref and TC\_ref powders. The distinguishable features of each components (Al, CuO, CuC and PVP molecules) are clearly observed. The CuC grains size is inhomogeneous and spans 30-100  $\mu\text{m}$  whereas Al and CuO particles are 80 and 100 nm in diameter, respectively. The dispersion of Al and CuO particles appears to be homogeneous in all inks: a good organization of Al and CuO nanoparticles around the big CuC grains (**Figure 3b, c, d, e & f**) is observed: white lines are drawn to localize them. In addition, the presence of the PVP binder enhances the cohesion of the Al, CuO and CuC particles. Indeed, on the inserts of **Figure 3a, b, c**, Al and CuO nanoparticles are well organized and packed. As indicated in the low-magnification images, **Figure 3a, b, c**, the Al is organised around CuO particles (~35–65 nm by 135-230 nm). Finally, increasing the quantity of PVP produces denser Al/CuO and CuC aggregates (**Figure 3c** compared to **Figure 3a**) in which reactants are completely drowned into the PVP.



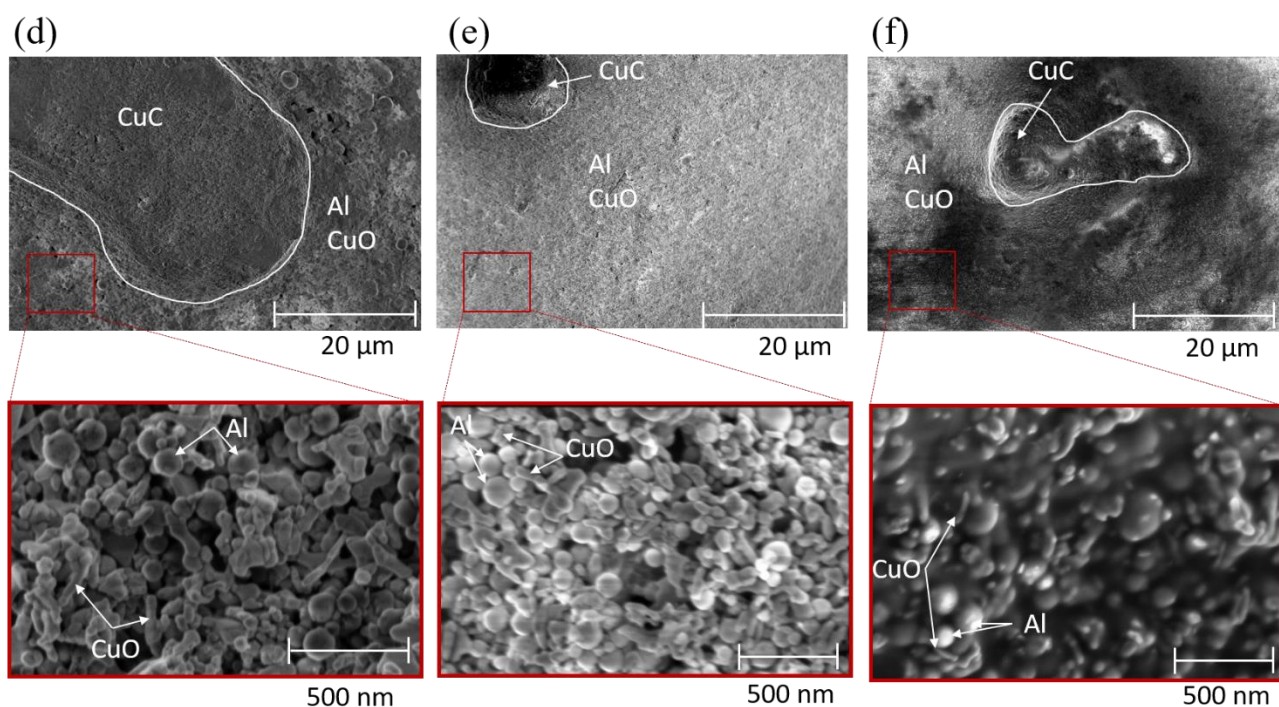


**Figure 3.** SEM images of Al/CuO\_ref (a + insert), TC\_ref (b + insert), TC\_3% (c + insert), TC\_5% (d + insert), TC\_10% (e + insert), TC\_25%(f + insert).

### 3.2. Influence of the mass fraction of PVP on the reactive materials combustion performances

To test the effects of PVP mass fraction on reactive inks, a series of samples was printed from various inks using the pneumatically driven syringe (**Figure 1b**) and then characterized for their combustion performances (flame temperature, pressure development and burning rate). From burning rate experiments, the average linear burn rate of each material is calculated and reported in **Figure 4a**. The burn rate decreases from 51 to 14 m/s as PVP mass fraction increases from 3 wt% to 7 wt%, which are more than 3 times slower than what obtained for Al/CuO/CuC mixture without PVP, *i.e.* TC\_ref (140 m/s). Generally, the reaction rate increases as the PVP content decreases. A coefficient of regression is calculated when applying an exponential fit to the burn rate results:  $r^2=0.976$ . Increasing the amount of PVP above 5 wt% in the ink rapidly

penalizes the combustion speed: it drops down to 7 m/s at 7 wt% of PVP and the flame quenches when it is above 7 wt%. Visual comparison of the burning rate are presented in **Figure 5**.

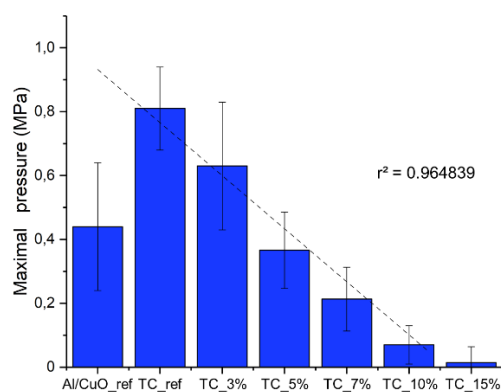
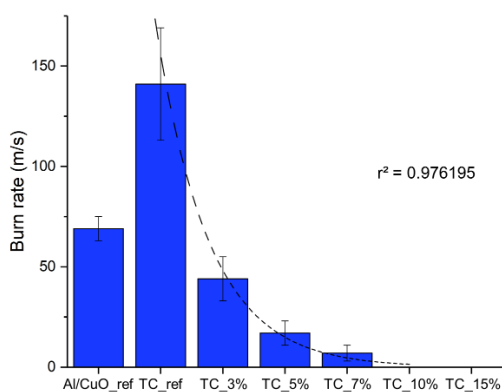
The temporal pressure records of the different reactive material samples are presented in supplementary file **Figure S3**. Pressure results in terms of maximal pressure and pressurization rate are summarized in **Figure 4b, c**. As expected, the results are in accordance with the burn rate characterizations: the highest pressure and pressurization rates are obtained with the TC\_ref material, *i.e.* without the polymer (0.8 MPa and 280 MPa/s). Increasing the mass fraction of PVP in the mixture has the effect to decrease the pressure generation performance linearly ( $r^2 = 0.96$ ).

TC\_3% produces 0.6 MPa and 250 MPa/s against 0.2 MPa and 90 MPa/s for TC\_7%. For higher polymer content, the pressure drops down to 0.07 MPa for TC\_10% and 0.01 MPa for TC\_15%. Below 5 wt%, PVP has only a slight impact on pressurization rate (decrease of ~10 %) which was not the case for burn rates and pressure. Nevertheless, for comparison, the maximal pressure generated by the TC with 3 wt% and less is double of those developed by a Al/CuO thermite characterized in the same conditions.

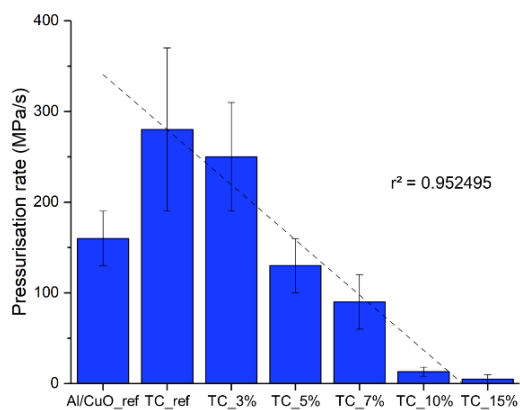
The calculated flame temperature (**Figure 4d**) is  $\sim 2800 \pm 60$  K and is independent of the polymer content. It is above the Al vaporization point (2740 K) and the Al<sub>2</sub>O<sub>3</sub> melting point (2345 K).

(a)

(b)



(c)



(d)

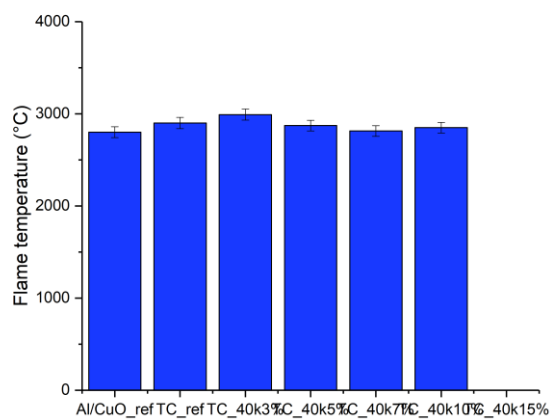


**Figure 4.** (a) Burn rate, (b) maximal pressure, (c) pressurization rate and (d) flame temperature as a function of the PVP content.

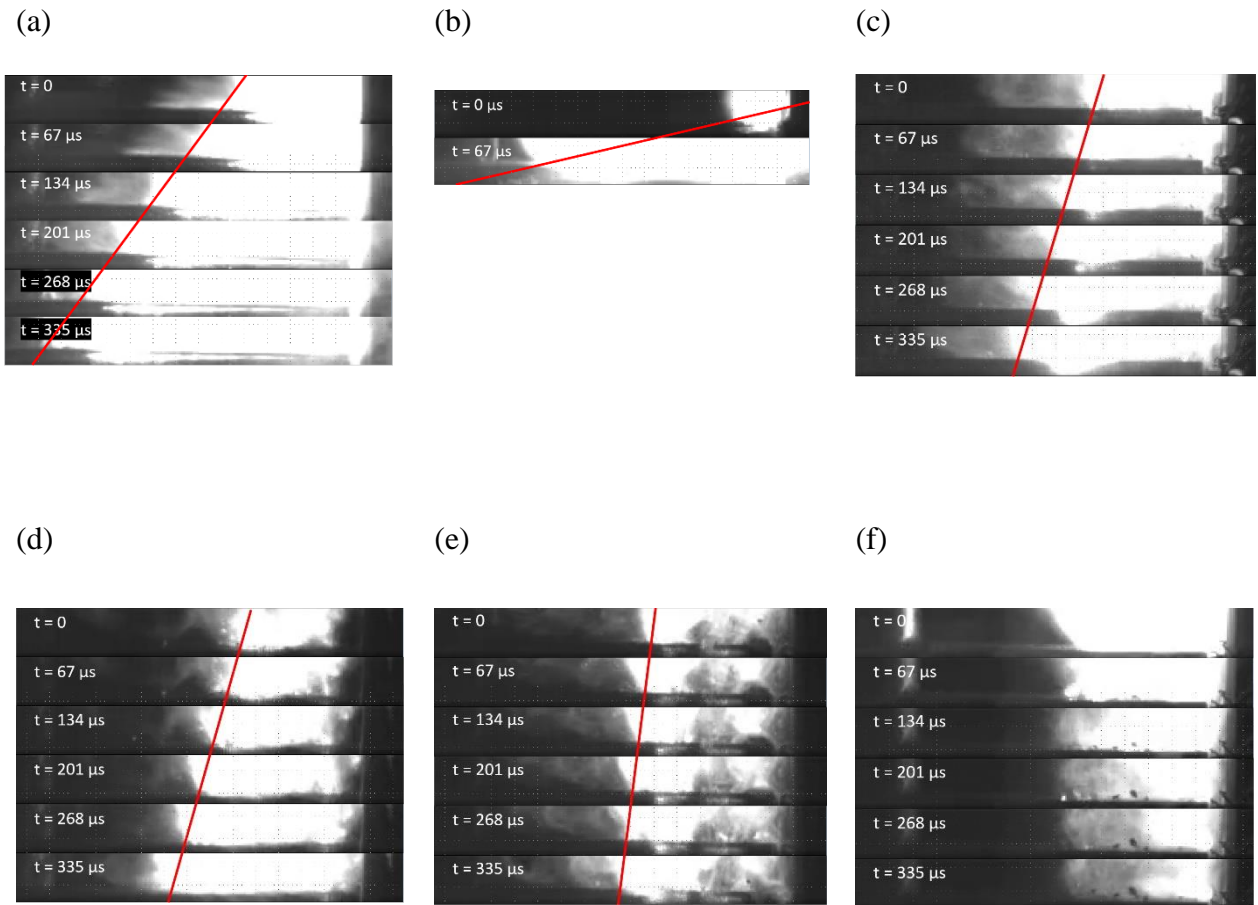


**Figure 5.** High-speed video images recorded for (a) Al/CuO<sub>ref</sub>, (b) TC<sub>ref</sub>, (c) TC<sub>3%</sub>, (d) TC<sub>5%</sub>, (e) TC<sub>7%</sub>, (f) TC<sub>10%</sub>. Each image is composed of 6 frames separated by 67  $\mu\text{s}$  except for TC<sub>ref</sub> which burns faster and contains only 2 frames. Total burning length is 3 cm.

The combustion tests lead to the conclusion that the mass fraction of PVP limits the overall reaction rate. Logically the thermite reaction should not be inhibited when the binding agent is a small fraction. The reduction of CuO and dissociation of CuC molecules first take place thanks to the initiation energy and is then sustained through an instantaneous reaction through the heat produced by the exothermic Al oxidation. At low PVP content, its effect on the reaction steps is negligible. Increasing the PVP content over 7 wt%, the CuO and CuC dissociation, which are both endothermic and require large activation energies to be self-sustained, failed. As a result, beyond 7 wt% PVP in Al/CuO/CuC reactive ink, the polymer inhibits the reaction by creating

radicals with lower energy than needed to continue the reaction. This analysis was confirmed by a complementary investigation based on differential scanning calorimetry (DSC) summarized in supplementary file **Figure S4**. For a polymer mass fraction below 7 wt%, the DSC traces feature a first exothermic peak around 270 °C corresponding to the CuC decomposition followed by the two main exotherms (around 575 and 780 °C) corresponding to the Al+CuO redox reaction as previously described <sup>36</sup>. The signature of PVP in DSC is represented by an endotherm at ~85 °C corresponding to its glass transition temperature which occurs well below the exothermic reactions and therefore does not impact the material decomposition. Increasing the PVP mass fraction beyond 7 wt%, the first exotherm is shifted to lower temperature: 550 °C (instead of 575 °C) and the second exotherm disappears. Increasing the PVP mass fraction > 10 wt% (TC\_10% and TC\_25%) no more exotherm is detected in the DSC traces. XRD patterns of the products collected after the DSC experiments (**Figure S5**) indicate that CuC has totally decomposed but Al and CuO have not. This confirms the inhibition of the reaction by the polymer.

For a PVP mass fraction < 7 wt%, the reactive prints remain highly reactive and self-propagate at high velocity (> 10 m/s) which was one important searched goal in this study. Note that 10 m/s is a decade faster than the majority of works dealing with printed energetic formulations featuring combustion speed well below 1 m/s <sup>43,28</sup>.

A PVP mass fraction of 5 wt% is therefore chosen to prepare printable Al/CuO/CuC reactive inks and characterize the prints (dropwise and continuously writing) produced by the two writing methods represented in **Figure 1b, c**: volumetrically controlled dispenser and pneumatically actuated syringe.

### 3.3 Reactive materials writing

**Figure 6a, b** demonstrates representative images of linear writing and dropwise writing of contiguous films. **Figure 6c, d** summarizes the average mass and diameter of the dried prints

as a function of the number of droplets injected in the same position. **Table S2** provides the detailed characteristic of the droplets printed drop by drop using the two writing methods. The minimum size of one droplet printed with the volumetrically controlled dispenser is slightly larger in size than the one written by the pneumatically actuated syringe. For the former case, the mass and size of a single droplet are about 1.14 mg and 3.3 mm; for the latter, 0.84 mg and 3.1 mm respectively. The mass and droplet size increase linearly with number of prints from 1 mg to > 10 mg. When six consecutive single droplets are deposited in the same position, a larger droplet is formed: its mass and diameter is of 6.96 mg, 9.3 mm (pneumatically actuated syringe) and 5.17 mg, 8.4 mm (volumetrically controlled dispenser).

A major concern of printing or writing applied to energetic materials is the consistency of the prints as it can lead to combustion instabilities and even quenching. The presence of bubbles or voids can typically create instabilities: as the reaction front encounters a void, the heat will be transported by convection whereas in dense media the main transport mechanism will be conduction. Hence, inhomogeneities will lead to velocities variation at the microscale as described in <sup>44</sup>. In addition, the presence of bubbles, if they are big, can lead to pressurization inside the material which may induce cracking and even disintegration of the film. As shown in **Figure S6** giving optical images of the printed material cross section show no inhomogeneity in the print at the microscale.

Finally, it is also observed on **Figure 6a** that the volumetrically controlled dispenser achieves cleaner and better defined contiguous film: the line width precision using the volumetrically controlled dispenser is  $\pm 0.5$  mm against  $\pm 1.1$  mm using the pneumatically actuated syringe. As the ink is liquid (viscosity  $\sim 1.5$  mP.s), using the pneumatic actuated syringe, it is sometimes hard to avoid leakage of droplets or even the syringe gets blocked after a few seconds as the ink dries in the needle which makes this solution unsuitable especially for continuous deposition. The volumetrically controlled syringe driver solves all these technical issues as the ink is totally

isolated from the outside air. When the ink output volume is set to 6  $\mu\text{l}$ , a single droplet fell. Under the condition that the output speed of the syringe was set to 30  $\mu\text{L}/\text{min}$ , the time between 2 droplets writing is 12 s.

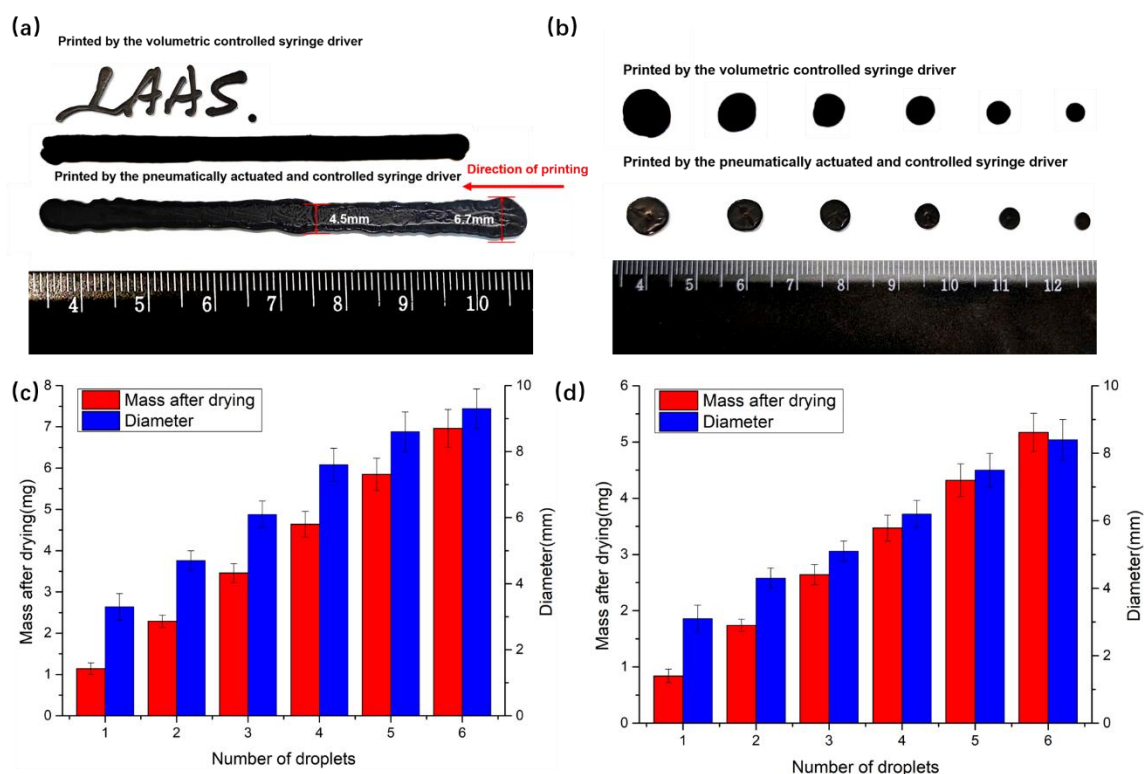


**Figure 6.** (a) Representative photographs of linear writing and (b) dropwise writing results obtained using the volumetrically controlled dispenser and pneumatically actuated syringe. Average diameter and mass of the droplets printed (c) with volumetrically controlled dispenser and (d) with pneumatically actuated syringe as a function of droplets.

#### 4. Conclusion

Stable Al/CuO/Cu<sub>2</sub>C reactive inks were developed using polymeric PVP binder. PVP presents the advantage to be biocompatible and widely used in MEMS technology. The PVP mass fraction in the reactive ink greatly impacts the combustion performances of the printed materials. The open-air burn rate decreases from 51 to 14 m/s as PVP mass fraction increases from 3 to 7 wt%. With 7 wt% of PVP in the ink, the combustion speed drops down to 7 m/s. The combustion fails propagating when PVP content is above 7 wt%. Pressure development

results are similar : increasing the mass fraction of PVP in the reactive ink has the effect to decrease the pressure generation performance linearly. Adding 3 and 7 wt% of PVP reduces the pressure generation by 25% and 80%, respectively in comparison with Al/CuO/CuC mixture without PVP. For higher polymer content, the pressure drops by 90%. But, the maximal pressure generated by a Al/CuO/CuC ink with 3 wt% PVP remains the double of those developed by a simple Al/CuO thermite characterized in the same condition. In this study, the optimized reactive ink i.e. that can be printed in contiguous layer by a volumetrically controlled dispenser or pneumatically actuated syringe, was found to contain 5 wt% of PVP polymer and 95 wt% Al/CuO/CuC powder. The printing (dropwise and continuously writing) produced by the volumetrically controlled dispenser achieves cleaner and better defined contiguous film: the line width precision is  $\pm 0.5$  mm against  $\pm 1.1$  mm using the pneumatically actuated syringe.

#### ASSOCIATED CONTENT

**Supporting Information.** The following files are available free of charge: more experimental details of home-made closed bomb setup and characterization data of Al/CuO, thermite composite, reactive inks and printed droplets.

#### AUTHOR INFORMATION

##### **Corresponding Author**

Carole Rossi, E-mail: [rossi@laas.fr](mailto:rossi@laas.fr), phone: 05 61 33 63 01

##### **Author contributions**

F.S. prepared all reactive materials inks and samples, performed all characterization measurements. X.L. and F.S. developed the direct writing process for both methods. T.W. synthesized CuC and assisted F.S. in the inks preparation. F.M. assisted F.S. in choosing the binder, setting up the ink preparation, and viscosity measurements. B.F. developed the software

controlling the injection parameter. S.A-S assisted F.S. and X.L. in the direct writing bench preparation. X.D. designed and fabricated the close bomb chamber. C.R. provided support for the manuscript preparation and supervised this research.

### **Funding Sources**

C.R. received funding from the European Research Council (ERC) under the European Union's Horizon 2020 research and innovation program (grand agreement No. 832889 - PyroSafe).

### **Competing financial interests**

The authors declare no competing financial interests.

### **ACKNOWLEDGMENT**

The authors acknowledge support from the European Research Council (H2020 Excellent Science) Researcher Award (grant 832889 – PyroSafe). This work was also supported by LAAS-CNRS technology platform, a member of Renatech network. We acknowledge the French Defense Agency DGA which partially funds F.S. scholarship and the China Scholarship Council which funds X.L. scholarship.

### **REFERENCES**

1. Aumann, C. E.; Skofronick, G. L.; Martin, J. A. Oxidation Behavior of Aluminum Nanopowders. *J Vac Sci Technol B* 1995, *13* (3), 1178-1183.
2. Stamatis, D.; Dreizin, E. L. Thermal Initiation of Consolidated Nanocomposite Thermites. *Combust Flame* 2011, *158* (8), 1631-1637.
3. Pantoya, M. L.; Granier, J. J. Combustion Behavior of Highly Energetic Thermites: Nano versus Micron Composites. *Propell Explos Pyrot* 2005, *30* (1), 53-62.
4. Martirosyan, K. S.; Wang, L. Z.; Vicent, A.; Luss, D. Nanoenergetic Gas-Generators: Design and Performance. *Propell Explos Pyrot* 2009, *34* (6), 532-538.
5. Rossi, C. Al-based Energetic Nanomaterials : Design, Manufacturing, Properties and Applications. Wiley: London, 2015; Vol. 2.
6. Chaalane, A.; Rossi, C.; Esteve, D. The Formulation and Testing of New Solid Propellant Mixture (DB plus x%BP) for a new MEMS-based Microthruster. *Sensor Actuat a-Phys* 2007, *138* (1), 161-166.
7. Staley, C. S.; Raymond, K. E.; Thiruvengadathan, R.; Apperson, S. J.; Gangopadhyay, K.; Swaszek, S. M.; Taylor, R. J.; Gangopadhyay, S. Fast-Impulse Nanothermite Solid-Propellant Miniaturized Thrusters. *J Propul Power* 2013, *29* (6), 1400-1409.

8. Rossi, C.; Larangot, B.; Pham, P. Q.; Briand, D.; de Rooij, N. F.; Puig-Vidal, M.; Samitier, J. Solid Propellant Microthrusters on Silicon: Design, Modeling, Fabrication, and Testing. *J Microelectromech S* 2006, 15 (6), 1805-1815.
9. Bezmelnitsyn, A.; Thiruvengadathan, R.; Barizuddin, S.; Tappmeyer, D.; Apperson, S.; Gangopadhyay, K.; Gangopadhyay, S.; Redner, P.; Donadio, M.; Kapoor, D.; Nicolich, S. Modified Nanoenergetic Composites with Tunable Combustion Characteristics for Propellant Applications. *Propell Explos Pyrot* 2010, 35 (4), 384-394.
10. Nicollet, A.; Salvagnac, L.; Bajot, V.; Estève, A.; Rossi, C. Fast Circuit Breaker based on Integration of Al/CuO Nanothermites. *Sensors and Actuators A: Physical* 2018, 273, 249-255.
11. Fleck, T. J.; Ramachandran, R.; Murray, A. K.; Novotny, W. A.; Chiu, G. T. C.; Gunduz, I. E.; Son, S. F.; Rhoads, J. F. Controlled Substrate Destruction Using Nanothermite. *Propell Explos Pyrot* 2017, 42 (6), 579-584.
12. Rossi, C. Engineering of Al/CuO Reactive Multilayer Thin Films for Tunable Initiation and Actuation. *Propellants, Explosives, Pyrotechnics* 2019, 44 (1), 94-108.
13. Zapata, J.; Nicollet, A.; Julien, B.; Lahiner, G.; Esteve, A.; Rossi, C. Self-propagating Combustion of Sputter-Deposited Al/CuO Nanolaminates. *Combust Flame* 2019, 205, 389-396.
14. Nicollet, A.; Lahiner, G.; Belisario, A.; Souleille, S.; Djafari-Rouhani, M.; Esteve, A.; Rossi, C. Investigation of Al/CuO Multilayered Thermite Ignition. *J Appl Phys* 2017, 121 (3).
15. de Koninck, D. A.; Briand, D.; de Rooij, N. F. A Shadow-Mask Evaporated PyroMEMS Igniter. *J Micromech Microeng* 2011, 21 (10).
16. Murray, A. K.; Novotny, W. A.; Fleck, T. J.; Gunduz, I. E.; Son, S. F.; Chiu, G. T. C.; Rhoads, J. F., Selectively-Deposited Energetic Materials: A Feasibility Study of the Piezoelectric Inkjet Printing of Nanothermites. *Addit Manuf* 2018, 22, 69-74.
17. Rodriguez, G. A. A.; Suhard, S.; Rossi, C.; Esteve, D.; Fau, P.; Sabo-Etienne, S.; Mingotaud, A. F.; Mauzac, M.; Chaudret, B. A Microactuator Based on the Decomposition of an Energetic Material for Disposable Lab-on-Chip Applications: Fabrication and Test. *J Micromech Microeng* 2009, 19 (1).
18. Adams, D. P. Reactive Multilayers Fabricated by Vapor Deposition: A Critical Review. *Thin Solid Films* 2015, 576, 98-128.
19. Abdallah, I.; Zapata, J.; Lahiner, G.; Warot-Fonrose, B.; Cure, J.; Chabal, Y.; Esteve, A.; Rossi, C. Structure and Chemical Characterization at the Atomic Level of Reactions in Al/CuO Multilayers. *ACS Applied Energy Materials* 2018, 1 (4), 17-62.
20. Blobaum, K. J.; Wagner, A. J.; Plitzko, J. M.; Van Heerden, D.; Fairbrother, D. H.; Weihs, T. P. Investigating the Reaction Path and Growth Kinetics in CuO<sub>x</sub>/Al Multilayer Foils. *J Appl Phys* 2003, 94 (5), 2923-2929.
21. Huang, C.; Jian, G. Q.; DeLisio, J. B.; Wang, H. Y.; Zachariah, M. R. Electrospray Deposition of Energetic Polymer Nanocomposites with High Mass Particle Loadings: A Prelude to 3D Printing of Rocket Motors. *Adv Eng Mater* 2015, 17 (1), 95-101.
22. Muravyev, N. V.; Monogarov, K. A.; Schaller, U.; Fomenkov, I. V.; Pivkina, A. N. Progress in Additive Manufacturing of Energetic Materials: Creating the Reactive Microstructures with High Potential of Applications. *Propell Explos Pyrot* 2019, 44 (8), 941-969.
23. Fleck, T. J.; Manship, T. D.; Son, S. F.; Rhoads, J. F. The Effect of Process Parameters on the Structural Energetic Properties of Additively Manufactured Reactive Structures. *Journal of Engineering Materials and Technology* 2020, 142 (4).
24. Zheng, D. W.; Huang, T. W.; Xu, B.; Zhou, X.; Mao, Y. F.; Zhong, L.; Gao, B.; Wang, D. J. 3D Printing of n-Al/Polytetrafluoroethylene-Based Energy Composites with Excellent Combustion Stability. *Adv Eng Mater* 2021.

25. Durban, M. M.; Golobic, A. M.; Bukovsky, E. V.; Gash, A. E.; Sullivan, K. T. Development and Characterization of 3D Printable Thermite Component Materials. *Adv Mater Technol-Us* 2018, 3 (12), 1800120.
26. Wainwright, E. R.; Sullivan, K. T.; Grapes, M. D. Designer Direct Ink Write 3D-Printed Thermites with Tunable Energy Release Rates. *Adv Eng Mater* 2020, 22 (6), 1901196.
27. Sullivan, K. T.; Zhu, C.; Duoss, E. B.; Gash, A. E.; Kolesky, D. B.; Kuntz, J. D.; Lewis, J. A.; Spadaccini, C. M. Controlling Material Reactivity Using Architecture. *Adv Mater* 2016, 28 (10), 1934-+.
28. Mao, Y. F.; Zhong, L.; Zhou, X.; Zheng, D. W.; Zhang, X. Q.; Duan, T.; Nie, F. D.; Gao, B.; Wang, D. J. 3D Printing of Micro-Architected Al/CuO-Based Nanothermite for Enhanced Combustion Performance. *Adv Eng Mater* 2019, 21 (12).
29. Ruz-Nuglo, F. D.; Groven, L. J. 3-D Printing and Development of Fluoropolymer Based Reactive Inks. *Adv Eng Mater* 2018, 20 (2).
30. Fleck, T. J.; Murray, A. K.; Gunduz, I. E.; Son, S. F.; Chiu, G. T. C.; Rhoads, J. F. Additive manufacturing of multifunctional reactive materials. *Addit Manuf* 2017, 17, 176-182.
31. Collard, D. N.; Fleck, T. J.; Rhoads, J. F.; Son, S. F. Tailoring the reactivity of printable Al/PVDF filament. *Combust Flame* 2021, 223, 110-117.
32. Meeks, K.; Pantoya, M. L.; Apblett, C. Deposition and characterization of energetic thin films. *Combust Flame* 2014, 161 (4), 1117-1124.
33. Clark, B.; Zhang, Z. H.; Christopher, G.; Pantoya, M. L. 3D processing and characterization of acrylonitrile butadiene styrene (ABS) energetic thin films. *J Mater Sci* 2017, 52 (2), 993-1004.
34. Wang, H. Y.; Shen, J. P.; Kline, D. J.; Eckman, N.; Agrawal, N. R.; Wu, T.; Wang, P.; Zachariah, M. R. Direct Writing of a 90 wt% Particle Loading Nanothermite. *Adv Mater* 2019, 31 (23).
35. Shen, J. P.; Wang, H. Y.; Kline, D. J.; Yang, Y.; Wang, X. Z.; Rehwoldt, M.; Wu, T.; Holdren, S.; Zachariah, M. R. Combustion of 3D printed 90 wt% loading reinforced nanothermite. *Combust Flame* 2020, 215, 86-92.
36. Wu, T.; Sevely, F.; Julien, B.; Sodre, F.; Cure, J.; Tenailleau, C.; Esteve, A.; Rossi, C. New Coordination Complexes-Based Gas-Generating Energetic Composites. *Combust Flame* 2020, 219, 478-487.
37. Wu, T.; Lahiner, G.; Tenailleau, C.; Reig, B.; Hungria, T.; Estève, A.; Rossi, C. Unexpected Enhanced Reactivity of Aluminized Nanothermites by Accelerated Aging. *Chem Eng J* 2021, 418, 129432
38. Wang, Z. Y.; Liu, J. S.; Ren, T. L.; Liu, L. T. Fabrication of Organic PVP Doping-Based Ba<sub>0.5</sub>Sr<sub>0.5</sub>TiO<sub>3</sub> Thick Films on Silicon Substrates for MEMS Applications. *Sensor Actuat a-Phys* 2005, 117 (2), 293-300.
39. Santra, S.; Hu, G.; Howe, R. C. T.; De Luca, A.; Ali, S. Z.; Udrea, F.; Gardner, J. W.; Ray, S. K.; Guha, P. K.; Hasan, T. CMOS Integration of Inkjet-Printed Graphene for Humidity Sensing. *Sci Rep-Uk* 2015, 5.
40. Biazar, E.; Roveimiab, Z.; Shahhosseini, G.; Khataminezhad, M.; Zafari, M.; Majdi, A. Biocompatibility Evaluation of a New Hydrogel Dressing Based on Polyvinylpyrrolidone/Polyethylene Glycol. *Journal of biomedicine & biotechnology* 2012, 2012, 343989.
41. Glavier, L.; Taton, G.; Ducere, J. M.; Baijot, V.; Pinon, S.; Calais, T.; Esteve, A.; Rouhani, M. D.; Rossi, C. Nanoenergetics as pressure generator for nontoxic impact primers: Comparison of Al/Bi<sub>2</sub>O<sub>3</sub>, Al/CuO, Al/MoO<sub>3</sub> nanothermites and Al/PTFE. *Combust Flame* 2015, 162 (5), 1813-1820.
42. Ng, D.; Fralick, G. Use of a multiwavelength pyrometer in several elevated temperature aerospace applications. *Rev Sci Instrum* 2001, 72 (2), 1522-1530.

43. Rehwoldt, M. C.; Wang, H.; Kline, D. J.; Wu, T.; Eckman, N.; Wang, P.; Agrawal, N. R.; Zachariah, M. R., Ignition and combustion analysis of direct write fabricated aluminum/metal oxide/PVDF films. *Combust Flame* 2020, *211*, 260-269.
44. Julien, B.; Wang, H. Y.; Tichtchenko, E.; Pelloquin, S.; Esteve, A.; Zachariah, M. R.; Rossi, C. Elucidating the dominant mechanisms in burn rate increase of thermite nanolaminates incorporating nanoparticle inclusions. *Nanotechnology* 2021, *32* (21).

# Table of Contents (TOC) graphic

